Effect of the interaction layer on the mechanical properties of Ti–6Al–4V alloy castings

Effect of the interaction layer on the mechanical properties of Ti-6Al-4V alloy castings

G. Q. Wu[1,*], X. Cheng[1], W. Sha[2], X. J. Cheng[1], J. Q. Zhao[3], H. Nan[3]

[1]School of Materials Science and Engineering, Beihang University, Beijing 100191, China

[2]School of Planning, Architecture and Civil Engineering, Queen's University Belfast, Belfast BT7 1NN, UK

[3]Beijing Institute of Aeronautical Materials, Beijing 100095, China

*Corresponding author: Tel: +86 1082313240; E-mail: guoqingwu@buaa.edu.cn

Abstract

The interaction between the face coat material of a mould and the titanium alloy will cause oxygen penetration during the casting and solidification process, resulting in the formation of an α-case interaction layer at the metal surface that influences the mechanical properties of the cast components. In this study, the influence of α-case thickness and loading positions in a Ti-6Al-4V (Ti64) alloy on metal hardness, impact properties and bending strength was investigated. The results showed that the metal surface α-case consisted of many coarse α laths which has a higher hardness than metal matrix. The mechanical properties of the alloy are influenced by the α-case. The alloy bending strength was observed to have changed linearly with the thickness of sample.

Keywords: hardness; optical microscopy; mechanical testing; solidification

1. Introduction

Ti-6Al-4V (Ti64) is one of the most widely used titanium alloys in the world. Because of its superior mechanical properties, corrosion resistance and biocompatibility, it is often used in aerospace, automobile and medical applications [1, 2]. Ti64 alloy is a typical α + β titanium alloy that consists of α and β laths in a Widmanstätten microstructure. Al and V in this alloy are mainly used to stabilise the α and β phases, respectively, and also improve the material ductility and strength [3]. The strength of Ti-6Al-4V alloy after annealing is around 800 MPa. After further heat treatment, the

strength of the alloy can reach around 1000 MPa, with excellent ductility [4, 5]. Ti-6Al-4V alloy also shows excellent oxidation resistance at temperatures around 200 °C. When the temperature reaches around 400 °C, the alloy starts to form a discontinued oxidation layer at the metal surface and gradually loses its oxidation resistance [6, 7].

However, the reactivity of this kind of alloy is very high, especially in its molten state. During the high temperature casting process, molten Ti64 will react with mould material. The oxygen from the mould face coat is diffused into the alloy. Because oxygen is a strong α phase stabiliser, an α phase layer is generated at the metal surface during metal solidification (α-case) [8]. Because it contains a large amount of oxygen, this surface α-case layer is hard, brittle and facilitates crack generation and propagation [9]. Over the years, much research has been carried out to improve the chemical inertness of mould face coat to reduce the α-case thickness [10]. Li et al. [11] studied the chemical inertness of ZrO_2 and Al_2O_3 face coats against molten Ti alloy. They found not only oxygen but also mould materials such as Zr and Al to penetrate into the alloy. Another study, carried out by Kartavykh et al. [12] illustrated that, when using boron nitride based face coat, a 30-50 μm interaction layer which contained a large amount of B and N formed at the titanium alloy surface. Meanwhile, the reaction between metal and alloy will also increase the surface roughness, reducing wear resistance, corrosion resistance and mechanical resistance [13, 14]. Fatigue failure was mostly generated from the surface contamination layer [15].

In order to understand the influence of the α-case layer on the mechanical properties of Ti64 alloy, research was carried out in this study to analyse the effect of α-case thickness and loading conditions on bending strength and properties. The hardness and fracture surface microstructures were also analysed.

2. Methodology

2.1. Material preparation

The composition of the cast Ti-6Al-4V material is shown in Table 1. Alloy was cast in moulds with yttria as the face coat material. In order to obtain a uniform α-case layer thickness, the cast was designed as a tube shape using a ZrO_2 cuboid core at the centre

of the tube (Figure 1). Therefore, the interaction between the metal and core would lead to an α-case layer at the tube inner surface. Then, the cast was machined into 60×10 mm plates with 2, 3 and 4 mm thickness, keeping one side with α-case layer, in preparation for further tests.

Table 1. Composition of the Ti64 cast titanium alloy (wt.%)

Al	V	Fe	Si	C	N	H	O
6.40	3.98	0.06	0.02	0.014	0.006	0.002	0.17

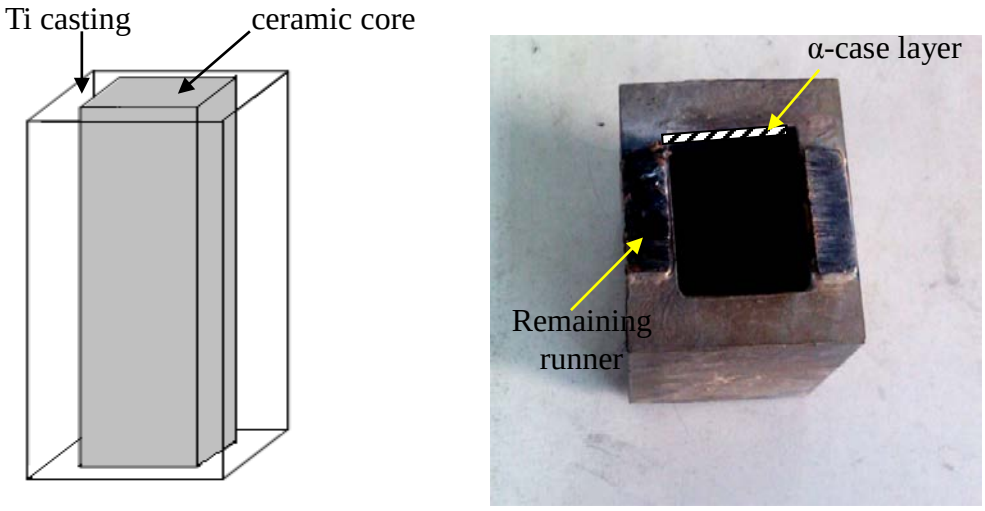

(a) (b)

Figure 1. The shape of the casting cuboid tube used in this experiment. (a) Schematic of casting shape; (b) the casting after removal of the internal core.

2.2. Microstructure observation

The microstructure of the metal was observed using an Olympus BX51M optical microscope. Samples were carefully ground, polished and etched using a 96 ml H_2O, 3 ml HNO_3 and 1 ml HF Kroll solution for around 20 s. Then, 1% NH_4F water solution was used to reveal the α-case layer. Fracture surfaces were observed using a JSM-4200 scanning electron microscope (SEM).

2.3. Mechanical testing

Three-point bending test was carried out using a universal testing machine (INSTRON 5565) with the loading speed of 0.2 mm/s. The dimension of the samples is 60×10 mm

with thickness of 2, 3 and 4 mm. During the bending test, samples were loaded in two different directions, one with α-case facing the load to bear compressive stress, and other with α-case opposite to the load to bear tensile stress (Figure 2). Cast samples without α layer were tested for comparison.

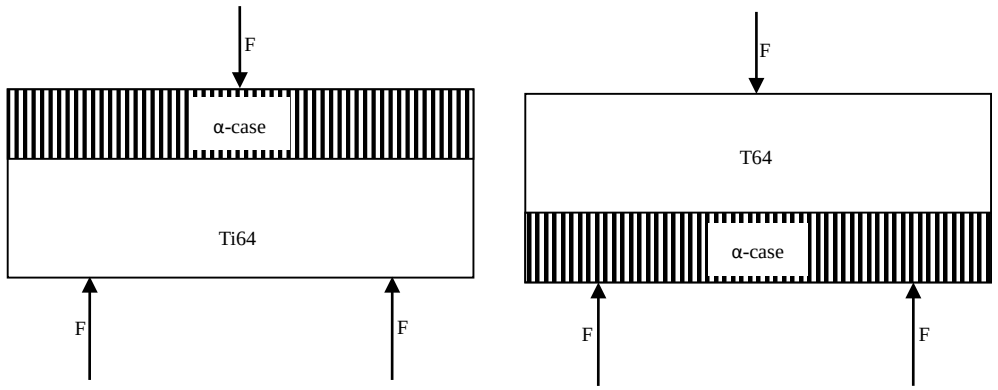

(a) (b)

Figure 2. Schematic diagram of the loading directions of the test samples. (a) α-case layer under compression; (b) α-case layer under tension.

The flexural stress σ and strain ε of the specimen can be obtained based on the following equations:

$$\sigma = \frac{3PL}{2bd^2} \quad (1)$$

$$\varepsilon = \frac{6Dd}{L^2} \quad (2)$$

where P is load at given point on the load deflection curve (N), L is the support span (40 mm), b is the width of the specimen (mm), d is the depth of the test beam (mm), D is the maximum deflection of the centre of the beam (mm).

Charpy impact testing was carried out using a JBS-750 digital display impact tester with pendulum impact energy of around 750 J. Samples with dimension of 55×10×3 mm were prepared without notch. The average total impact energy can be obtained from the equipment after the tests from five samples.

The hardness was measured using a HXZ 1000 hardness tester with 50 g indent loading. The indentations were made in the metal with spacing of around 50 μm from the metal surface to the metal matrix at around 0.8 mm. The hardness of the metal at each distance was then calculated from the average value of 10 indentations.

3. Results

3.1. Microstructure of the α-case at the metal surface

Due to the metal/core interaction, an obvious α-case was formed at the metal surface with a thickness of around 0.35 mm (Figure 3). As can be seen, the α-case layer at the metal surface is brighter compared to the metal matrix. It consists of many coarse α laths and no grain boundaries can be recognised in the α-case layer. For the metal matrix, the obvious α + β lamellar structure was observed, with different grain orientations.

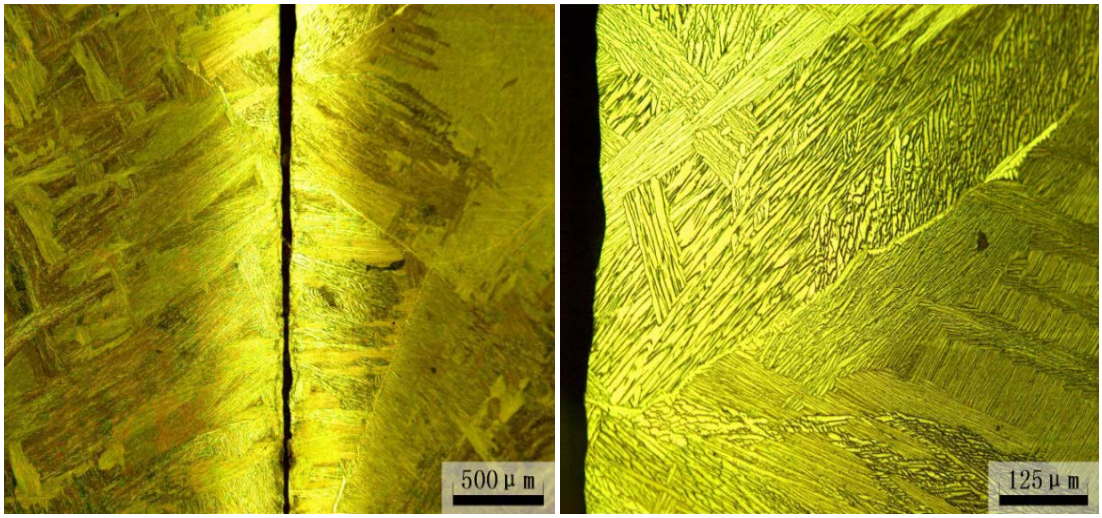

(a) (b)

Figure 3. Optical microstructure of the inner surface in the square tube casting. (a) Low magnification, (b) high magnification.

3.2. Hardness

The hardness of the Ti-6Al-4V was measured from the surface to the metal matrix (Figure 4). As can be seen, the hardness of the metal matrix was around 380 HV. A very high hardness of around 590 HV was obtained at the metal surface. The hardness gradually decreases as the distance from the metal surface increases to level off at approximately 380 HV at a depth of around 0.4 mm.

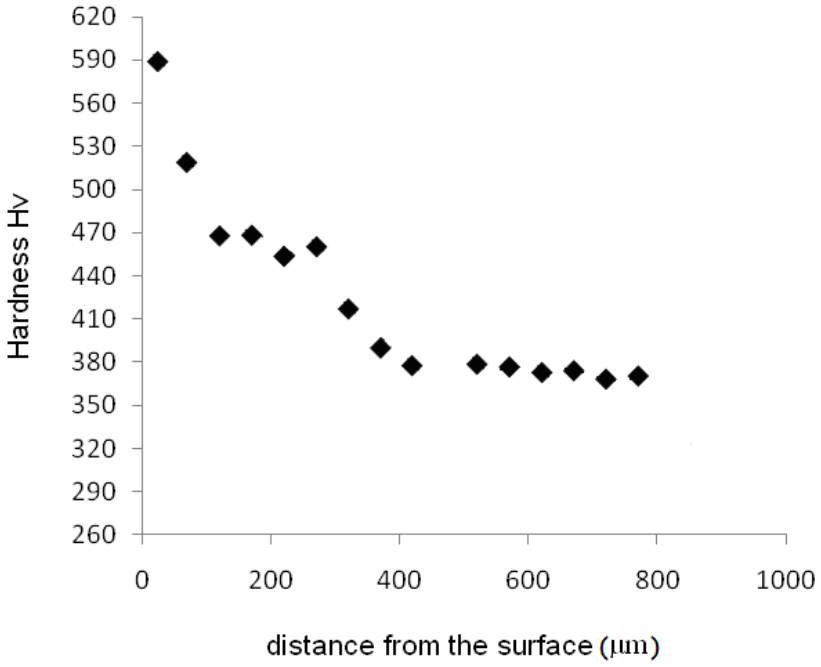

Figure 4. Hardness profile of the metal from the surface inwards.

3.3. Bending test

Three point bending test was carried out in this study to understand the influence of sample thickness and loading direction on the mechanical properties of components. Samples with thickness of 2 mm, 3 mm and 4 mm were used in this test with different α-case proportion through the thickness (Figure 5).

The ultimate strength of samples 2 mm in thickness without α-case layer was 1410 MPa (average value from five samples as used in Figure 5b and not from the individual test specimen shown in Figure 5a) with total strain of around 10%. For samples in which the α-case layer was subjected to compressive stress, they broke after the ultimate strength of around 1570 MPa, reaching a smaller total strain of 7%. However, for samples with the α-case layer subjected to tension, they show brittle failure during elastic deformation with the maximum stress around 710 MPa and strain of around 3%. The stress-strain curves for other specimen thicknesses have similar shapes as those shown in Figure 5a, but with different strength levels as given in Figure 5b.

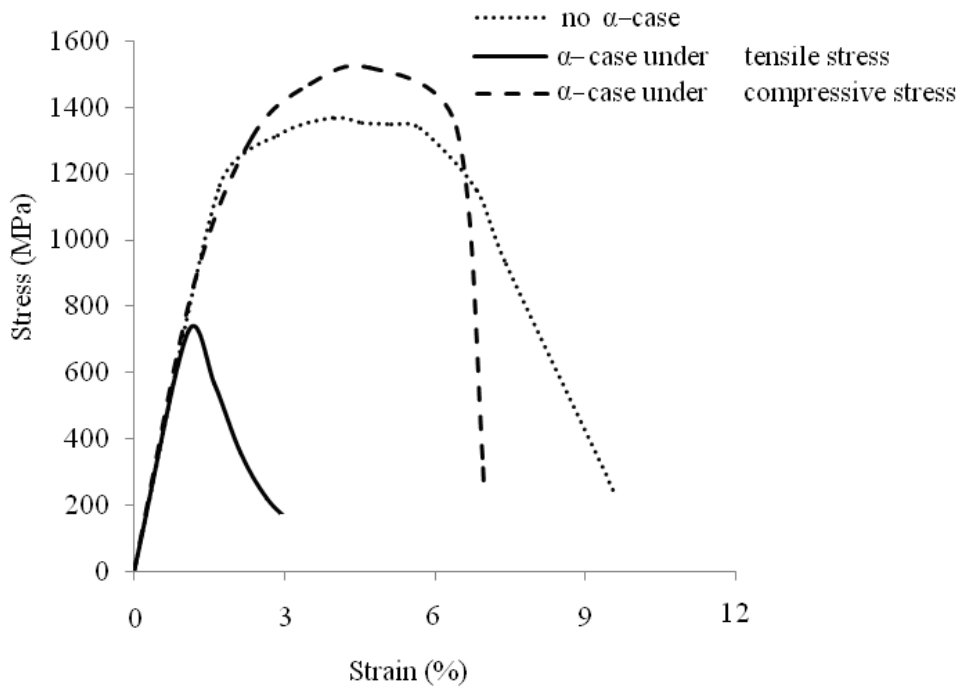

(a)

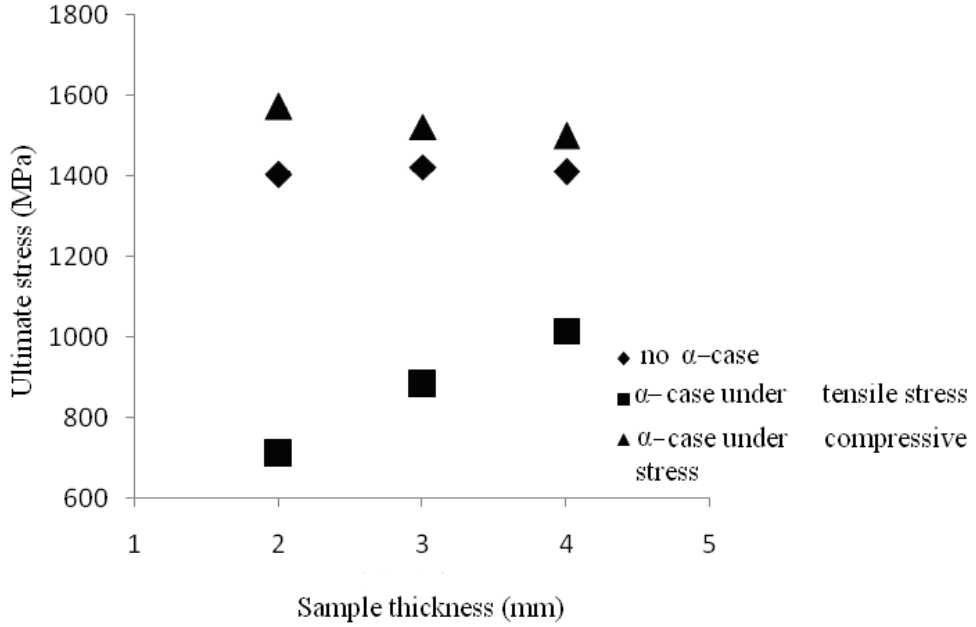

(b)

Figure 5. Bending properties with different loading directions. (a) Calculated stress-strain curves of 2 mm samples; (b) the average ultimate strength.

When samples did not contain α-case, the increase of sample thickness from 2 mm to 4 mm did not influence the ultimate strength. The average strength was around 1410 MPa

(Figure 5b). However, when containing α-case, the bending strength of a sample of 2 mm thickness was changed to 1570 MPa and 710 MPa when the α-case was subjected to compressive stress and tensile stress, respectively. The increase in sample thickness to 4 mm (decreasing α-case layer proportion) when the α-case was under tensile stress led to a dramatic increase in material strength from 710 MPa to 1020 MPa. For the samples in which the α-case was under compressive stress, the decrease of α-case proportion in sample led to a decrease of bending strength from 1570 MPa to 1500 MPa.

3.4. Microstructure of the fracture surface

The fracture surfaces after bending test are shown in Figure 6. As can be seen, for the samples in which the α-case was subjected to tensile stress, the fracture plane shows growth along a direction perpendicular to the sample surface to around 0.5-0.6 mm to the metal matrix. As was known, the α-case thickness in the metal surface was 0.35 mm, indicated by a dashed line in each micrograph in Figure 6. Therefore, it appears that the crack started to nucleate in the α-case and then grew through the α-case to the metal matrix and caused the final failure of the material. However, for samples in which the α-case was subjected to compressive stress, the fracture plane was found to be inclined at an angle of about 45° to the loading axis, and the grain structure of the metal can be observed at the fracture surface, above the dashed lines in Figures 6c and 6d. Hence, the crack growth in these samples was closely related to the grain structure, resulting in a longer crack growth path and higher strength. However, because of the embrittlement of the α-case, after reaching the ultimate strength, further deformation will lead to a quick failure. In this study, the changes of sample thickness were not observed to influence their fracture morphology.

3.5. Impact toughness

Due to the different location of α-case layer, the impact behaviour was different (Figure 7). The casting without α layer has the largest impact energy, 35.3 J, splitting to 15.5 J and 19.8 J for parts before and after the peak in Figure 7, respectively. For samples containing α-case layer, the impact properties were deteriorated. For the samples where the α-case layer faced the impact force, the total energy absorption is reduced to 29.9 J, splitting to 13.1 J and 16.8 J for parts before and after the peak in Figure 7, respectively.

However, when α-case was opposite to the impact loading, a large reduction of the impact energy was observed, to 7.5 J, reducing by nearly 80% compared to the sample without α-case. Samples were broken immediately once a crack was generated.

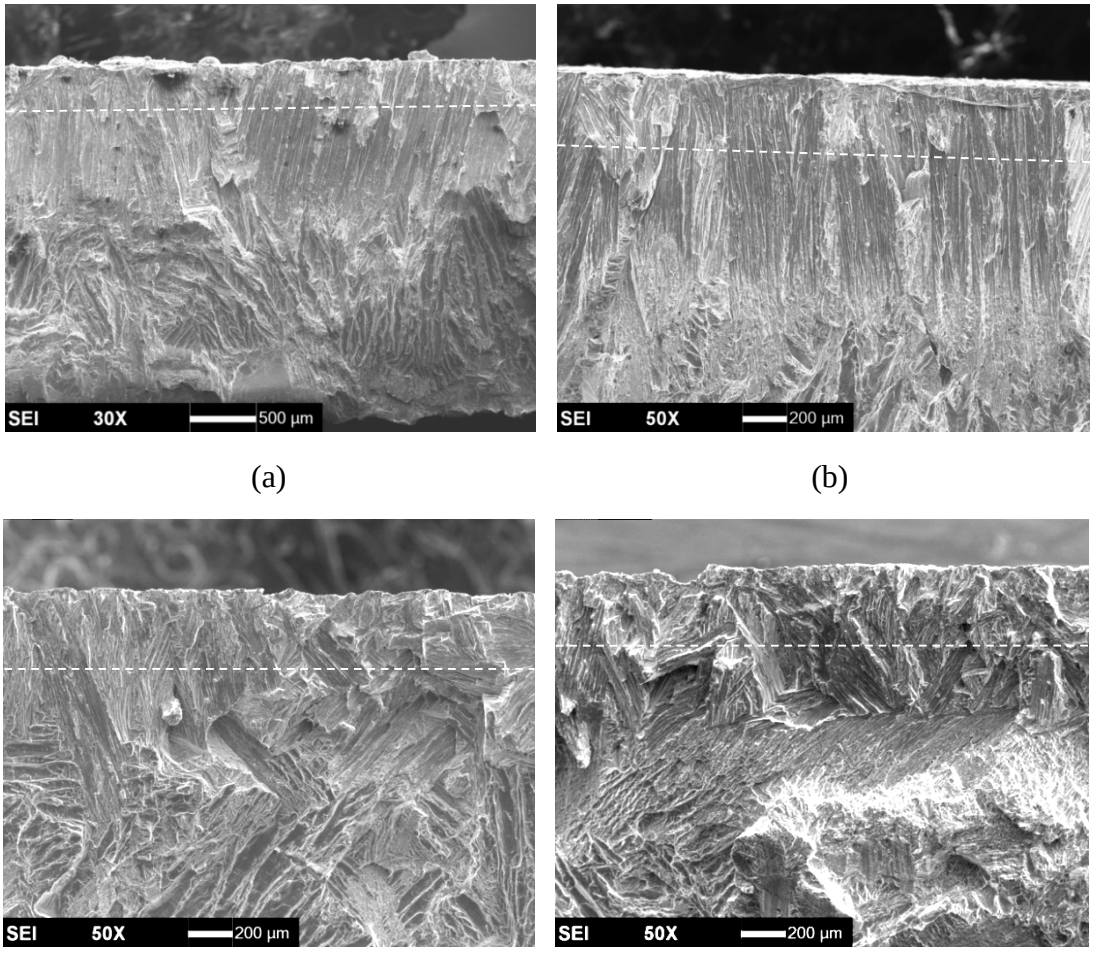

Figure 6. SEM micrographs of fracture surface of the bending test samples. (a) 2 mm sample with α-case side under tensile stress; (b) 4 mm sample with α-case side under tensile stress; (c) 2 mm sample with α-case side under compressive stress; (d) 4 mm sample with α-case side under compressive stress. In each fractograph, the top part, above approximately the dashed line, is the α-case.

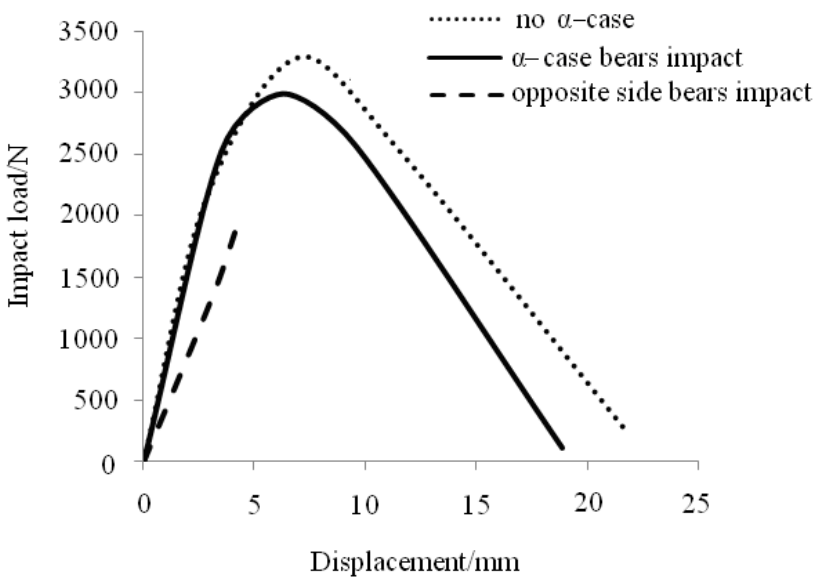

Figure 7. Load–displacement curves of the 3 mm testing samples under impact.

4. Discussion

4.1. Microstructure of the α-case layer

It can be seen from Figure 3 that the interaction between the mould and molten Ti64 alloy will lead to an α-case layer forming at the metal/core interface with coarse α laths growth from the metal surface. In this experiment, the average α-case thickness was around 0.35 mm. Because of the solid solution hardening by the dissolved oxygen of the metal at the metal/core interface, it shows a high hardness (Figure 4). As the distance away from the metal surface increased, the metal hardness gradually dropped from 590 HV to around 380 HV, with the hardened layer thickness of around 0.4 mm.

4.2. Influence of α-case on alloy mechanical properties

The three-point bending test results shown in Figure 5b illustrate that the increase of sample thickness from 2 mm to 4 mm does not influence bending strength. The average bending strength of the material was around 1410 MPa. When the sample contained an α-case layer, the bending strength was changed from 1410 MPa to 1570 MPa when the α-case layer was under compressive stress and from 1410 MPa to 710 MPa when the α-case layer was under tensile stress, for a sample of 2 mm thickness. Meanwhile, the change of sample thickness will also influence the bending strength. When the α-case was under tensile stress, the decrease of sample thickness led to a dramatic decrease of

bending strength. However, for the sample in which the α-case was under compressive stress, the decrease of sample thickness led to an increase of bending strength. The sample thickness had a larger impact on bending strength when the α-case was under tensile stress. The ratio of sample thickness to α-case thickness affects the bending strength.

The impact toughness was also influenced by the α-case layer. The sample without α-case had total energy absorption of 35.3 J during impact test. When samples contained α-case and the α-case was facing the impact force, a reduction of the impact energy was detected, by around 15%. For samples in which the α-case was opposite to the incoming impact force, once the crack formed, the sample immediately broke with a large reduction in energy of around 80%.

The different mechanical properties with or without an α-case layer were closely dependent on the mechanical properties of the α-case layer. The surface α-case layer contains a large amount of oxygen in solid solution. Oxygen atoms occupy the interstitial sites leading to the change in ductility and hardness [16]. Because the α-case appears at the metal surface, it serves as the stress raisers that eventually cause the oxygen-rich zone to crack, leading to the failure of the alloy at lower strain [17, 18]. When the α-case was subjected to tensile force and impact tensile force, the cracks were first nucleated in the α-case layer and propagated very quickly through, resulting in brittle failure. When the α-case layer was subjected to compressive force, the crack was first generated in the metal matrix and then propagated through, until it caused failure. The failure in the case of compressive stress appears like brittle failure.

5. Conclusions

The microstructure of the α-case on the metal/core surface consists of many coarse α laths with a thickness of around 0.35 mm. Due to the presence of the α-case, the hardness of the alloy at the casting surface was around 590 HV. The measured hardened layer thickness at the metal surface was around 0.4 mm.

During bending, when the α-case layer was under tensile stress, a large reduction of bending strength was observed, and the bending strength was decreased with decreased sample thickness (increased α-case proportion). The cracks were first nucleated in the α-case and grew very quickly through the sample. When the α-case at the surface was under compressive stress, a slightly increased bending strength was observed when sample thickness was decreased.

The impact energy was largely reduced when containing an α-case layer, especially when the α-case was facing away from the incoming impact.

Acknowledgements

This paper is financially supported by the Aeronautics Fundamental Science Foundation of China (2012ZE51056) and the Cheung Kong Scholars and Innovative Research Team Program in University from the Ministry of Education (Grant No. IRT0805).

References

[1] M. Peters, J. Hemptenmacher, J. Kumpfert, C. Leyens, in: C. Leyens, M. Peters (Eds.), Titanium and Titanium Alloys, Wiley-VCH Verlag, 2005, pp. 1-36.

[2] H.P. Nicolai, C. Liesner, in: C. Leyens, M. Peters (Eds.), Titanium and Titanium Alloys, Wiley-VCH Verlag, 2005, pp. 263-271.

[3] M. Niinomi, Mater. Sci. Eng. A 243 (1998) 231-236.

[4] G. Lütjering, Mater. Sci. Eng. A 243 (1998) 32-45.

[5] B.D. Venkatesh, D.L. Chen, S.D. Bhole, Mater. Sci. Eng. A 506 (2009) 117-124.

[6] H. Guleryuz, H. Cimenoglu, J. Alloy. Compd. 472 (2009) 241-246.

[7] S. Kumar, T.S.N. Sankara Narayanan, S. Ganesh Sundara Raman, S.K. Seshadri, Mater. Chem. Phys. 119 (2010) 337-346.

[8] S.Y. Sung, Y.J. Kim, Mater. Sci. Eng. A 405 (2005) 173-177.

[9] L. Yue, Z. Wang, L. Li, Appl. Surf. Sci. 258 (2012) 8065-8071.

[10] Y. Guilin, L. Nan, L. Yousheng, W. Yining, J. Prosthet. Dent. 97 (2007)157-164.

[11] B.S. Li, A.H. Liu, H. Nan, W.S. Bi, J.J. Guo, H.Z. Fu, Trans Nonferrous Met. Soc. China 18 (2008) 518-522.

[12] A.V. Kartavykh, V.V. Tcherdyntsev, J. Zollinger, Mater. Chem. Phys. 119 (2010) 347-350.
[13] K.S. Chan, M. Koike, B.W. Johnson, T. Okabe, Metall. Mater. Trans. A 39 (2008) 171-180.
[14] C.E. Shamblen, T.K. Redden, in: R.I. Jaffee, N.E. Promisel (Eds.), The Science, Technology and Applications of Titanium, Pergamon, Oxford, 1970, pp. 199-208.
[15] R.W. Evans, R.J. Hull, B. Wilshire, J. Mater. Process. Technol. 56 (1996) 492-501.
[16] M. Lamirand, J. Bonnentien, S. Guérin, G. Ferrière, J. Chevalier, Metall. Mater. Trans. A 37 (2006) 2369-2378.
[17] S.N. Patankar, Y.T. Kwang, T.M. Jen, J. Mater. Process. Technol. 112 (2001) 24-28.
[18] W.C. Say, Y.Y. Tsai, Surf. Coat. Technol. 176 (2004) 337-343.